

Numerical study of simultaneous natural convection heat transfer from both surfaces of a uniformly heated thin plate with arbitrary inclination

J. J. Wei, B. Yu, H. S. Wang, W. Q. Tao

309

Abstract Numerical studies were conducted to investigate the natural convection heat transfer around a uniformly heated thin plate with arbitrary inclination in an infinite space. The numerical approach was based on the finite volume technique with a nonstaggered grid arrangement. For handling the pressure–velocity coupling the SIMPLE-algorithm was used. QUICK scheme and first order upwind scheme were employed for discretization of the momentum and energy convective terms respectively. Plate width and heating rate were used to vary the modified Rayleigh number over the range of 4.8×10^6 to 1.87×10^8 . Local and average heat transfer characteristics were compared with regarding to the inclination angle. The empirical expressions for local and average Nusselt number were correlated. It has been found that for inclination angle less than 10° , the flow and heat transfer characteristics are complicated and the average Nusselt number can not be correlated by one equation while for inclination angle larger than 10° , the average Nusselt number can be correlated into an elegant correlation.

List of symbols

g	gravitational acceleration (m/s^2)
h	heat transfer coefficient ($\text{W/m}^2 \cdot \text{K}^{-1}$)
k	thermal conductivity ($\text{W/m} \cdot \text{K}^{-1}$)
Nu	Nusselt number
p	pressure (N/m^2)
Pr	Prandtl number
q	natural convection heat flux (W/m^2)
q^*	uniform heat generation rate per unit area (W/m^2)
Ra^{**}	modified Rayleigh number based on uniform heat generation, defined by Eq. (14)
t	plate thickness (m)
T	temperature ($^\circ\text{C}$)

T_∞	bulk (ambient) fluid temperature ($^\circ\text{C}$)
u	fluid velocity component in x direction (m/s)
v	fluid velocity component in y direction (m/s)
W	plate width (m)
x	coordinate along the plate, $x = 0$ at the plate edge (m), Fig. 1
y	coordinate perpendicular to the plate (m), Fig. 1

Greek symbols

α	thermal diffusivity (m^2/s)
β	thermal expansion coefficient (K^{-1})
ν	kinematic viscosity (m^2/s)
θ	inclination angle of the plate with the horizontal ($^\circ$), Fig. 1
ρ	fluid density (kg/m^3)

Subscripts

av	average value
j	$j = \text{u, l}$ for the upper and lower plate surfaces respectively
l	lower plate surface
u	upper plate surface
w	plate value
x	local value

1

Introduction

Natural convective flow over heated surfaces appears in a variety of natural circumstances (thermal plumes, meteorological phenomena, etc.) as well as in many industrial applications (cooling of electronic circuit board, electric transformers, heated covering, veneer, etc.). Most work in these fields is devoted to the study of flat plate, one of the basic configurations typically addressed in natural convection heat transfer. McAdams [1] reported the experimental results of natural convection heat transfer for upward and downward facing isothermal surfaces. Hatfield and Edwards [2] experimentally studied natural convection from a downward facing horizontal isothermal plate, and measurements were made for square and rectangular plates in air, water and a high Prandtl number oil. The plate aspect ratio was accounted for in their correlations. Clifton and Chapman [3] analyzed the natural convection from a heated downward facing isothermal surface by the integral boundary layer approach. Kierkus [4] performed a perturbation solution for the velocity and temperature fields for laminar free convection about an inclined isothermal plate. The experimental research on the upward facing uniform heat flux surface were conducted by Sparrow and Carlson

Received on 18 April 2001 / Published online: 29 November 2001

J. J. Wei, B. Yu, W. Q. Tao (✉)
 School of Energy and Power Engineering
 Xi'an Jiaotong University
 Xi'an, Shaanxi 710049, China
 E-mail: wqtao@xjtu.edu.cn

H. S. Wang
 Institute of Advanced Material Study
 Kyushu University, Kasuga,
 Fukuoka 816-8580, Japan

Support from the National Key Project of Fundamental R&D of China (Grant No. G 2000026303) is greatly acknowledged.

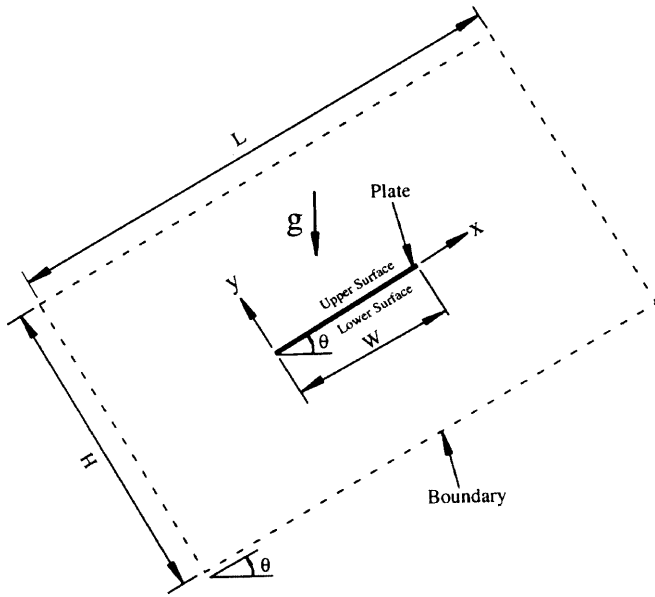


Fig. 1. Schematic of the physical model

[5]. There were many solutions of the boundary-layer equations on the free convection along a vertical surface with uniform heat flux [6, 7]. Referring to their results, Fujii and Fujii [8] proposed a simple and accurate expression of coefficient (function of fluid Prandtl number) in the correlation of local Nusselt number with the modified Rayleigh number. Natural convection heat transfer over an inclined plate is also of considerable interest to engineers because of its application to solar energy and cooling of electronic equipment. Fujii and Imura [9] made an average heat transfer coefficient measurement for an inclined heated plate, and in the laminar region the average heat transfer coefficient correlated reasonably well with vertical plate data if the gravitational term in the Grashof number was the component parallel to the heated surface. Their heated surface, however, neither isothermal nor of uniform heat flux as they claimed.

All the above researches were concentrated on natural convection heat transfer from a single side heated surface. For the case of concurrent heat transfer from both side surfaces of the heated plate, local heat transfer coefficients at each surface are difficult to obtain experimentally due to the necessity of having to determine the percentage of the total heat transfer rate being convected from each surface. Chambers and Lee [10] numerically studied the local and average natural convection Nusselt numbers for simultaneous convection above and below a uniformly heated horizontal thin plate.

For this case, the natural convection above the upward surface and that below the downward surface are coupled each other, and the percentage of the heat transfer rate from the two sides cannot be specified priori, rather, it is the result of the numerical computation, making the problem being of a conjugate type. The conjugate natural convection heat transfer characteristics of an inclined thin plate with uniform heat flux is very interesting and of great importance in applications, such as the packaging of microelectronic chips in the cooling of electronic circuit board, but have not been revealed in detail yet. For the cooling of electronic

board, the plates are usually situated in an enclosure. Symons et al. [11] experimentally studied the natural convection of two parallel isothermal plates in an isothermal cubic enclosure. The two plates were allowed to installed in any orientation inside the enclosure. They found that the existence of the enclosure had little effect on the overall heat transfer rates of the plates. Yang and Tao [12] experimentally found that the difference between the average Nusselt numbers of a vertical plate in a confined space and in the infinite space was trivial when the Rayleigh number is less than 10^6 . Therefore the study of natural convection in an infinite space may provide useful information for the design of cooling device of electronic equipment. As indicated before, because of the measurement difficulty, all the above experimental study only provide the plate averaged heat transfer coefficient, which is not enough for the design of electronic cooling device, where the most critical component should be positioned at the place with the highest local heat transfer coefficient. Therefore it motivates the authors to do the present numerical investigation to clarify the local natural convection heat transfer coefficient distribution characteristics at different inclination angle.

2

Numerical model

A schematic of the physical model is shown in Fig. 1. A two-dimensional thin plate was heated by embedding a uniform heat source (heat per unit area) within it, and surrounded by the air. The heated plate was modeled using a cuboid block element, which was discretized into 50 nodes along its width. The plate thickness was set at $1/50$ of the plate width and was discretized by only one node. The thermal conductivity of the plate was assumed to be $300 \text{ W/(m}^2 \cdot \text{K)}$, approximately 10000 times larger than the thermal conductivity of the air, thus the thermal resistance in the plate can be neglected compared with that of the air. To prevent unwanted conduction within the plate in x direction, thickless adiabatic internal wall elements were centered between successive pairs of plate nodes. Adiabatic walls were adopted at the plate ends. Two plate widths ($W = 0.0408$ and 0.102 m) and four heat fluxes ($q^* = 50, 100, 200, \text{ and } 500 \text{ W/m}^2$) were used in spanning the range of modified Rayleigh numbers investigated, $4.8 \times 10^6 \leq Ra^{**} \leq 1.87 \times 10^8$ (Ra^{**} defined in Eq. (14) below).

2.1

Governing equations

With the assumption of steady, two-dimensional laminar flow and constant properties for the air, using Boussinesq assumption to account for buoyancy effects, the governing equations for the fluid region are

$$\frac{\partial u}{\partial x} + \frac{\partial v}{\partial y} = 0 \quad (1)$$

Momentum equations

$$u \frac{\partial u}{\partial x} + v \frac{\partial u}{\partial y} = -\frac{1}{\rho} \frac{\partial p}{\partial x} + \nu \left(\frac{\partial^2 u}{\partial x^2} + \frac{\partial^2 u}{\partial y^2} \right) + \beta g \sin \theta (T - T_\infty) \quad (2)$$

$$u \frac{\partial v}{\partial x} + v \frac{\partial v}{\partial y} = -\frac{1}{\rho} \frac{\partial p}{\partial y} + \nu \left(\frac{\partial^2 v}{\partial x^2} + \frac{\partial^2 v}{\partial y^2} \right) + \beta g \cos \theta (T - T_\infty) \quad (3)$$

Energy equation

$$u \frac{\partial T}{\partial x} + v \frac{\partial T}{\partial y} = \alpha \left(\frac{\partial^2 T}{\partial x^2} + \frac{\partial^2 T}{\partial y^2} \right) \quad (4)$$

The governing equation within the solid plate is

$$\frac{\partial^2 T}{\partial x^2} + \frac{\partial^2 T}{\partial y^2} + \frac{q^*}{tk} = 0. \quad (5)$$

2.2

Solution domain and its boundary conditions

To study the natural convection heat transfer in an infinite space, a large enough finite solution domain should be selected such that further enlarge the space would not affect the results. A rectangular solution domain was adopted with the plate at the center as shown by the dashed line in Fig. 1. The size of the domain was determined by testing the effect of the domain size on average Nusselt number and maximum temperature rise. Horizontal and vertical plate cases with simultaneous convection over both of the plate surfaces were tested respectively. Table 1 shows the results at $Ra^{**} = 1.87 \times 10^7$. With a reasonable accuracy of the results, the size of the domain was assumed to be three times the plate width in x direction and twice the plate width in y direction.

Uniform temperature (ambient temperature) and static pressure (atmospheric pressure) were imposed at all the four boundaries of the solution domain.

2.3

Numerical methods

The finite volume method was adopted to discretize the governing equations. The SIMPLE algorithm was used for treating the coupling between velocity and pressure, and QUICK scheme and first order upwind difference scheme were used to discretize the convective terms in momentum and energy equations, respectively.

The grid was non-uniform, decreasing geometrically toward the ends and surfaces of the plate, resulting in an increasingly fine grid where large thermal and velocity gradients existed. The grid thickness adjacent immediately to the plate surfaces and ends was one half of the plate thickness. Within the solid, the grid was uniform. A grid sensitivity study was performed by varying the grid within the fluid. Figure 2 shows the results of maximum

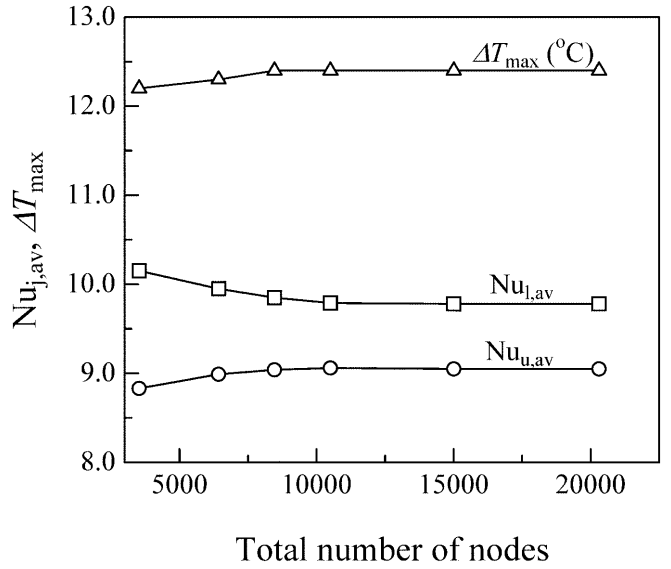


Fig. 2. Effect of grid number on the numerical results

temperature rise and average Nusselt number for each test case. The 102×103 grid yielded a temperature rise 0.1 percent smaller, a Nusselt number 0.05 percent and 0.3 percent larger for the upper surface and lower surfaces, respectively, compared to the finest grid (142×143). Thus the results of 102×103 grid were chosen as the solutions independent of the grid number.

3

Data reduction

The local heat flux was determined by following equation

$$q_{j,x} = -k \frac{\partial T_x}{\partial y} \bigg|_j \quad (6)$$

The local heat transfer coefficients and local Nusselt numbers were defined as

$$h_{j,x} = q_{j,x} / (T_{w,x} - T_\infty) \quad (7)$$

and

$$Nu_{j,x} = h_{j,x} W / k \quad (8)$$

where, $j = u$ and l for the upper and lower heated surfaces respectively. The plate width W was adopted as the characteristic length instead of the local coordinate x (Sparrow and Carlson, 1986), allowing the x -dependence of the Nusselt number to exhibit the same x -dependence as the local heat transfer coefficient.

The average heat flux and average plate temperature were defined as

$$q_{j,av} = \frac{1}{W} \int_0^W q_{j,x} dx \quad (9)$$

$$T_{w,av} = \frac{1}{W} \int_0^W T_{w,x} dx \quad (10)$$

Table 1. Effect of solution domain size on the numerical results

Test plate	$L/W \times H/W$	$Nu_{u,av}$	$Nu_{l,av}$	ΔT_{max} (°C)
Horizontal	2.0×1.5	8.282	9.510	12.93
	3.0×2.0	9.062	9.792	12.43
	4.0×3.0	9.065	9.822	12.41
Vertical	3.0×2.0	15.97	15.97	7.38
	4.0×3.0	16.06	16.06	7.19

The average heat transfer coefficients and average Nusselt numbers were then obtained as

$$h_{j,av} = \frac{q_{j,av}}{T_{w,av} - T_{\infty}} \quad (11)$$

and

$$Nu_{j,av} = h_{j,av} W / k \quad (12)$$

It is noticed here that Chambers and Lee [10] calculated the average heat transfer coefficient by performing the integration

$$h_{j,av} = \frac{1}{W} \int_0^W h_{j,x} dx \quad (13)$$

For the case of natural convection heat transfer around a uniformly heated plate, the above definition of average heat transfer coefficient appears inappropriate. This is because $T_{w,x} - T_{\infty}$ is not a constant, which makes the average heat transfer coefficient obtained from Eq. (13) inconsistent with that from Newton's law of cooling.

The Nusselt number is parameterized in terms of a modified Rayleigh number since a heat flux or heat generation rate was prescribed instead of a surface temperature. The modified Rayleigh number was defined as

$$Ra^{**} = \frac{g\beta q^* W^4}{\nu^2 k} Pr \quad (14)$$

where q^* is the uniform heat generation rate per unit area within the plate, and the summation of heat fluxes from both surfaces at a location x is equal to q^* .

Local modified Rayleigh number was defined as

$$Ra_{j,x}^{**} = \frac{g\beta q_{j,x} x^4}{\nu^2 k} Pr. \quad (15)$$

4

Results and discussion

For validation of the CFD code, some numerical tests were performed. First, numerical simulation was carried out for natural convection from a horizontal upward facing surface with uniform heat flux.

The behavior of local Nusselt numbers is shown in Fig. 3. Local Nusselt numbers have been normalized by sixth root of their corresponding Ra^{**} as $Nu_{u,x}/(Ra^{**})^{1/6}$ which are plotted against the dimensionless coordinate x/W . The dependence of $Nu_{u,x}/(Ra^{**})^{1/6}$ on x/W closely agrees with both the least squares fit correlation of Chambers and Lee [10] and the experimental data of Sparrow and Carlson [5]. The results of average Nusselt number versus Ra^{**} are shown in Fig. 4. The experimental data of Sparrow and Carlson [5] are also shown there for comparison. The 1/6-power dependence relates well with the experimental data and the maximum difference between simulated results and the experimental data is within 13.5 percent. The numerical simulation gives a least square fit correlation with forced slope of 1/6 as

$$Nu_{u,av} = 0.928(Ra^{**})^{1/6} \quad \text{for } 4.8 \times 10^6 \leq Ra^{**} \leq 1.87 \times 10^8 \quad (16)$$

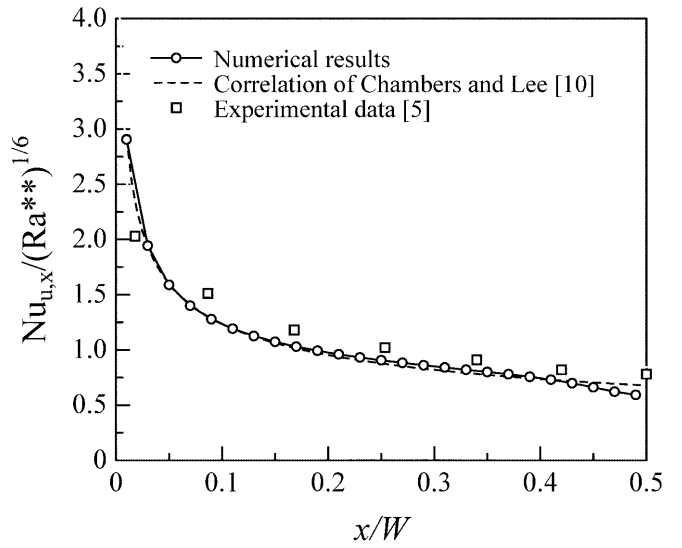


Fig. 3. Normalized local Nusselt number distribution along the plate width for a uniformly heated horizontally upward facing plate

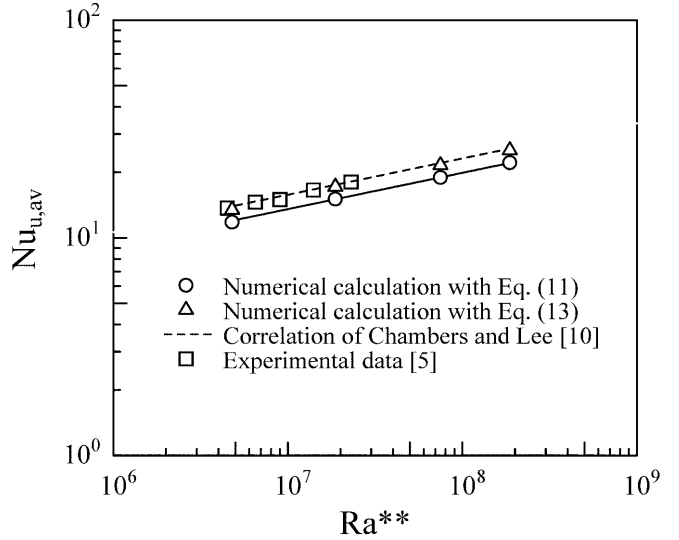


Fig. 4. Comparison of simulated and experimental Nusselt numbers for a horizontally upward facing uniformly heated plate

For comparison with the results of Chambers and Lee [10], the present numerical average Nusselt number with Eq. (13) and the correlation of Chambers and Lee [10] are also shown in Fig. 4. It is seen that a good agreement for the two results is obtained. The unfit definition of the average heat transfer coefficient by Eq. (13) results in an average Nusselt number around 13 percent larger than that by Eq. (11).

Secondly, numerical simulation was carried out for a uniformly heated vertical plate with simultaneous convection over the two surfaces. Figure 5 shows the results of local Nusselt number versus local modified Rayleigh number. A least square fit correlation of the data can be obtained as

$$Nu_{j,x}(x/W) = 0.531(Ra_{j,x}^{**})^{1/5} \quad \text{for } 10^5 \leq Ra_{j,x}^{**} \leq 1.87 \times 10^8 \quad (17)$$

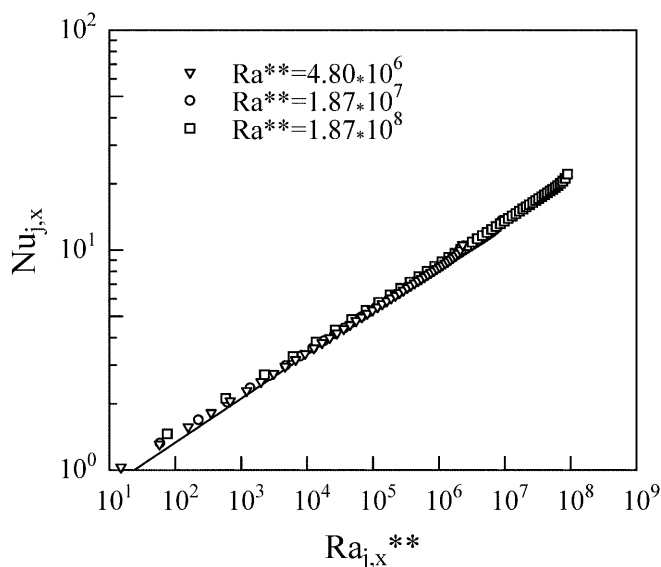


Fig. 5. Local Nusselt number versus local Rayleigh number for simultaneous convection from both surfaces of a uniformly heated vertical plate

The product of the left side in Eq. (17) is equivalent to the local Nusselt number defined by Fujii and Fujii [8]. The coefficient 0.531 is a little larger than that in the Fujii and Fujii correlation (0.519 for $Pr = 0.702$) obtained from the boundary layer theory. The small difference may be due to the edge effect which was not considered in the boundary layer theory.

With the above validations, presented in the following sections are the calculated results of the natural convection heat transfer for a uniformly heated plate with simultaneous convection over the two surfaces.

Figures 6 and 7 show typical examples of the vector pattern and isothermal lines around the heated thin plate for the inclination angles of 0, 3, 10, 20, 60 and 90° at $Ra^{**} = 1.87 \times 10^7$. For the horizontal position ($\theta = 0^\circ$), the two air streams move inward along the plate from the two opposite edges while tending to rise due to buoyancy. The farthest inward penetration of the streams is to $x = W/2$, where they collide and form an air plume upward. With increase of the inclination angle, due to the gravity component parallel to the heated surface, the position of the air plume is shifted from the center to the trailing edge of the plate.

Figure 8 shows typical examples of the local heat flux fraction from the two heated surfaces for the inclination angles of 0, 3, 10, 20, 60 and 90° at $Ra^{**} = 1.87 \times 10^7$. For the horizontal position, the local heat flux at the center of the lower surface is maximum and decreased toward the two edges, which is contrary to that of the upper surface, due to the difference of the development of boundary layer. With the inclination angle increasing, the local heat flux peaks are shifted toward the trailing edge, which agrees with the shift of air plume in Figs. 6 and 7. The local heat flux peaks disappear and the heat fluxes from the two surfaces become equal at $\theta = 90^\circ$ due to the symmetry.

Figure 9 shows typical examples of the average heat flux fraction $q_{j,av}/q^*$ from the two heated surfaces versus the

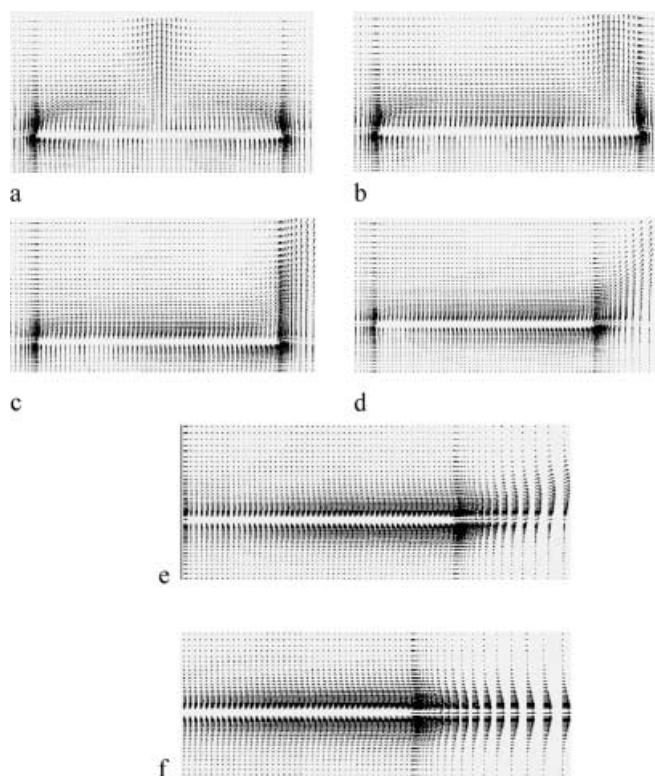


Fig. 6a-f. Velocity vector pattern around the plate. a $\theta = 0^\circ$; b $\theta = 3^\circ$; c $\theta = 10^\circ$; d $\theta = 20^\circ$; e $\theta = 60^\circ$; f $\theta = 90^\circ$

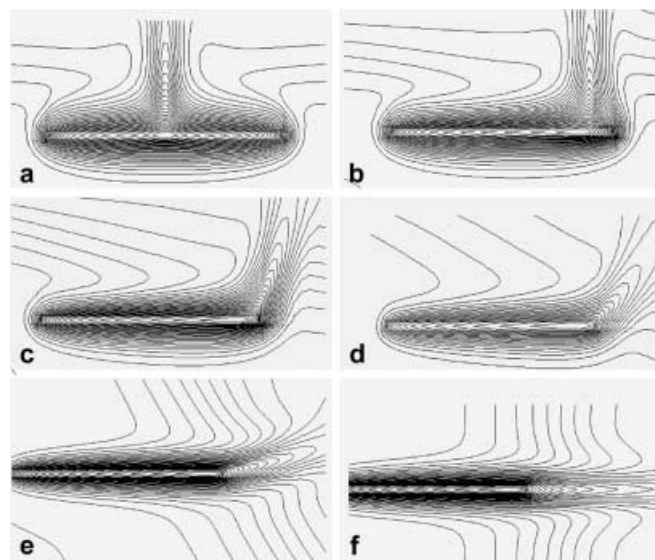


Fig. 7a-f. Isothermal lines around the plate. a $\theta = 0^\circ$; b $\theta = 3^\circ$; c $\theta = 10^\circ$; d $\theta = 20^\circ$; e $\theta = 60^\circ$; f $\theta = 90^\circ$

inclination angle θ at $Ra^{**} = 1.87 \times 10^7$. It can be clearly observed that as far as the average heat flux is concerned, the upward and downward surfaces have essentially almost the same averaged heat flux for inclination angle greater than 10°.

Figure 10 shows typical examples of the temperature distribution along the plate at $Ra^{**} = 1.87 \times 10^7$ for the inclination angles of 0, 3, 10, 20, 30, 60 and 90°. With the

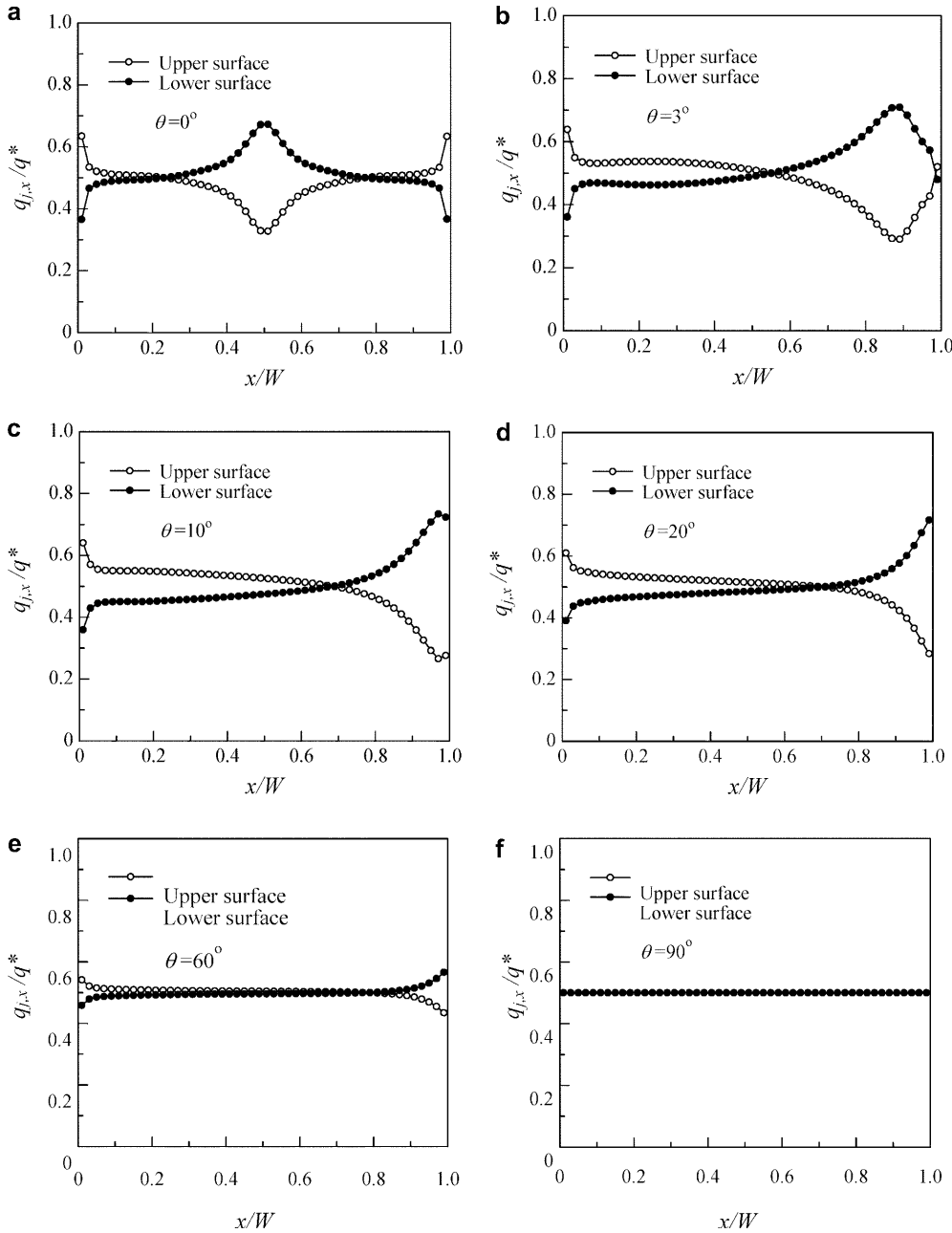


Fig. 8a-f. Local heat flux fraction from the upper and lower surfaces

increase of the inclination angle, just like the heat flux peaks, the temperature peak is shifted from the plate center toward the trailing edge. Decrease of average temperature shows that the natural convection heat transfer increases with the increase of the inclination angle and gets its best when the plate is vertical.

Figure 11 shows local Nusselt number normalized by their corresponding average Nusselt number, $Nu_{u,x}/Nu_{u,av}$, versus x/W for inclination angle of 0° – 90° . The normalized local Nusselt numbers for all the modified Rayleigh numbers investigated here collapse to one curve at the same inclination angle. Figure 11a shows the results for all the modified Rayleigh numbers, whereas only the results at $Ra^{**} = 1.87 \times 10^7$ are shown in the other figures for clarity.

For the upper surface at $\theta = 0^\circ$ (see Fig. 11a), the local Nusselt number decreases by power law variation from the

two edges of the plate to the center, and the correlation can be expressed as

$$\begin{cases} Nu_{u,x}/Nu_{u,av} = 0.670(x/W)^{-0.254} & x/W < 0.5 \\ Nu_{u,x}/Nu_{u,av} = 0.670(1-x/W)^{-0.254} & x/W \geq 0.5 \end{cases} \quad (18)$$

For the upper surface in the range $0^\circ < \theta \leq 20^\circ$ (see Fig. 11b), the local Nusselt number on the upper surface decreases by power law variation from the leading edge to the trailing edge, and the correlation can be expressed as

$$Nu_{u,x}/Nu_{u,av} = 0.770(x/W)^{-0.282} \quad (19)$$

For the lower surface in the range $0^\circ \leq \theta \leq 20^\circ$ (see Fig. 11c), the local Nusselt numbers decrease by power law variation from the two edges of the plate to the center, and the correlation can be expressed as

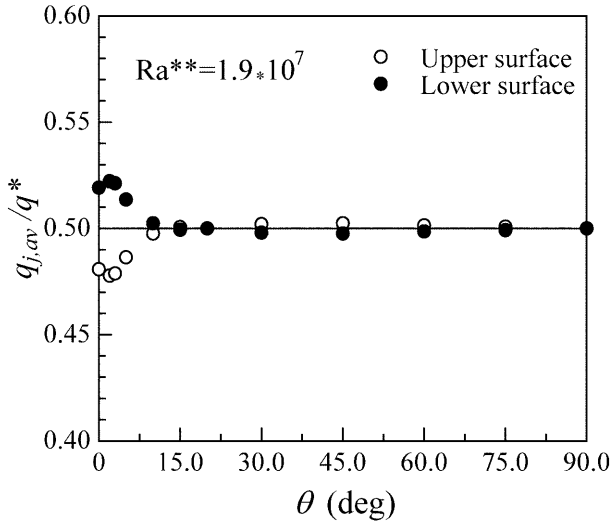


Fig. 9. Average heat flux fraction from the upper and lower surfaces

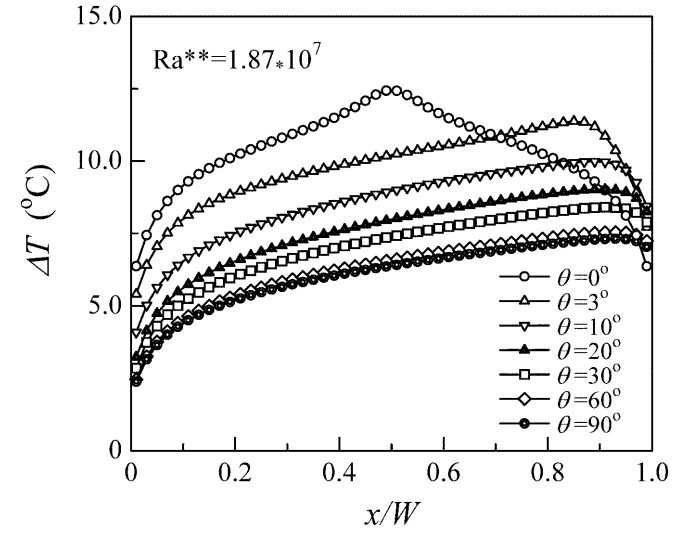


Fig. 10. Temperature distribution along the plate

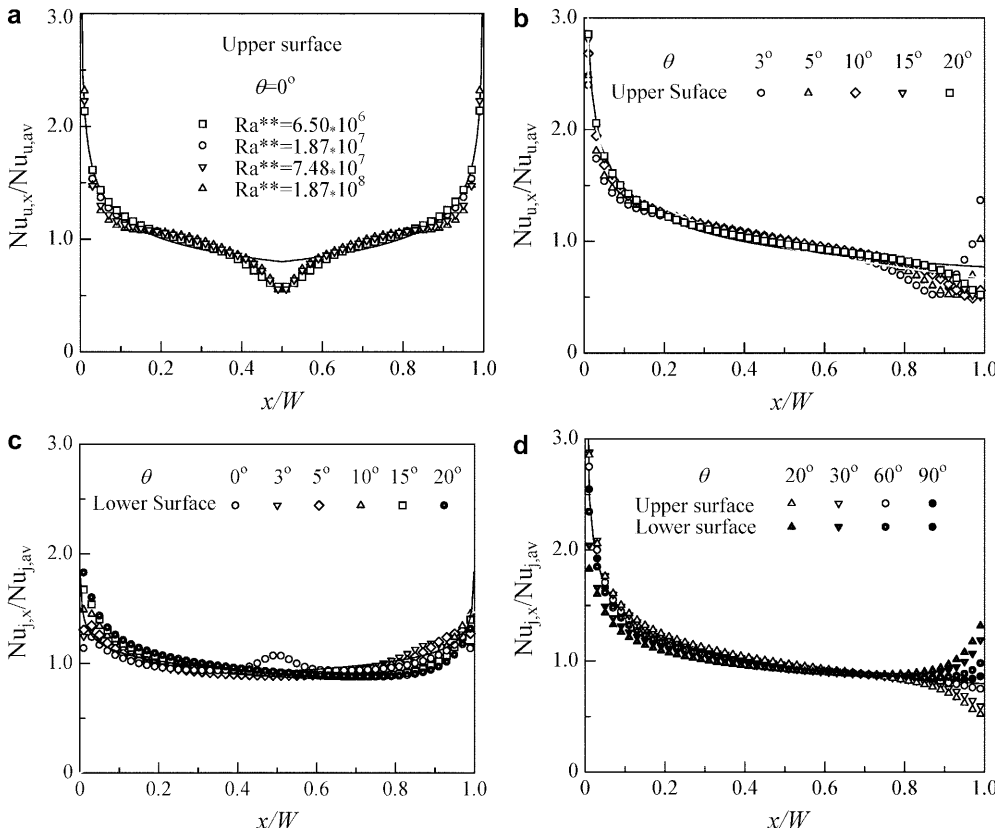


Fig. 11a-d. Normalized local Nusselt number distribution along the plate width. **a** $\theta = 0^\circ$ for the upper surface; **b** $0^\circ < \theta \leq 20^\circ$ for the upper surface; **c** $0^\circ \leq \theta \leq 20^\circ$ for the lower surface; **d** $20^\circ \leq \theta \leq 90^\circ$ for the upper and lower surfaces

$$\begin{cases} \text{Nu}_{l,x}/\text{Nu}_{l,av} = 0.856(x/W)^{-0.110} & x/W < 0.5 \\ \text{Nu}_{l,x}/\text{Nu}_{l,av} = 0.856(1 - x/W)^{-0.110} & x/W \geq 0.5 \end{cases} \quad (20)$$

For the upper and lower surfaces in the range $\theta \geq 20^\circ$ (see Fig. 11d), the local Nusselt number decreases by power law variation from the leading edge to the trailing edge, and a uniform correlation for both the upper and lower surfaces can be expressed as

$$\text{Nu}_{j,x}/\text{Nu}_{j,av} = 0.795(x/W)^{-0.25} \quad (21)$$

The above formula reveals that the local heat transfer coefficient is proportional to $x^{-0.25}$ for both the upper and lower heated surfaces, which agrees with the results obtained by boundary layer theory for free convection along a vertical single side heated surface with uniform heat flux [6, 7].

When the inclination angle $\theta \geq 20^\circ$, the gravity component parallel to the heated surface seems to become a dominant factor to determine the natural heat transfer in despite of the gravity component perpendicular to the heated surface. Thus the correlation of the local Nusselt

number for the inclination angle $\theta \geq 20^\circ$ can be expressed as nearly same formula for both the upper and lower heated surfaces; while those for the inclination angle $\theta < 20^\circ$, the gravity component parallel to the heated surfaces is not so large to play a dominant role, thus the conjugate natural convection heat transfer becomes very complicated, resulting in very different heat transfer of the upper and lower surfaces.

Figure 12a shows the effects of inclination angle and the modified Rayleigh number on average Nusselt numbers for the plate inclination angles of $0-90^\circ$. For the lower surface, the range of $0-10^\circ$ is magnified and shown in Fig. 12b for clear observation. For the inclination angle $\theta < 10^\circ$, the heat transfer characteristics of the upper and lower surfaces are different. Average Nusselt numbers on the upper and lower surfaces can be expressed as

$$Nu_{u,av} = [0.317 + 0.645(\sin \theta)^{1.18}](Ra^{**})^{0.2} \quad (22)$$

and

$$Nu_{l,av} = \{0.675(Ra^{**})^{-0.04} + [0.00293(Ra^{**})^{0.256} + 0.158] \sin \theta\}(Ra^{**})^{0.2} \quad (23)$$

for $4.8 \times 10^6 \leq Ra^{**} \leq 1.87 \times 10^8$, respectively.

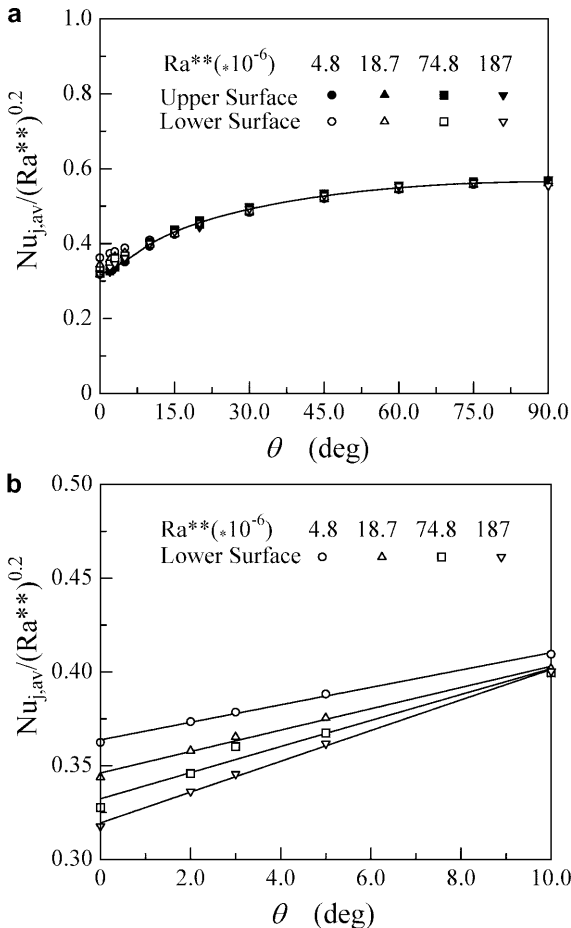


Fig. 12a, b. Effects of inclination angle and the modified Rayleigh number on average Nusselt number. **a** $0^\circ \leq \theta \leq 90^\circ$ for the upper and lower surfaces; **b** $0^\circ \leq \theta \leq 10^\circ$ for the lower surface

For $Ra^{**} \leq 7.5 \times 10^7$, average Nusselt number on the lower surface is larger than the corresponding Nusselt number on the upper surface and the difference between lower and upper Nusselt numbers decreased with the increase of Ra^{**} . This is due to the thickening of the upper surface boundary layer generated from the fluid being preheated by the lower surface [10].

Although the correlations of local Nusselt numbers for the inclination angle $10^\circ \leq \theta \leq 20^\circ$ are different for the upper and lower heated surfaces, average Nusselt number for the inclination angle $\theta > 10^\circ$, fortunately, can be nearly expressed with a same correlation for the two heated surfaces. They can be well correlated with the modified Rayleigh number, and the correlation keeps the same as the vertical plate if only the gravitational term in the modified Rayleigh number is altered to the component parallel to the inclined surface. The correlation can be expressed as

$$Nu_{j,av} = 0.565(Ra^{**} \sin \theta)^{0.2} \quad (24)$$

for $4.8 \times 10^6 \leq Ra^{**} \leq 1.87 \times 10^8$

5

Conclusions

The effect of inclination angle on the natural convection heat transfer from both surfaces of a volumetrically uniform heated thin plate with large thermal conductivity was investigated by numerical simulation. It is found that for inclination angle less than 20° , the local natural convection heat transfer is very different for the upper and lower heated surfaces. The local Nusselt number on the lower surface decreases by power law variation from the two edges of the plate to the center, whereas the local Nusselt number on the upper surface decrease by power law variation from the leading edge to the trailing edge except for the horizontal surface. For inclination angle greater than 20° , the local Nusselt number normalized by the corresponding average Nusselt number is almost same for both the heated surfaces, decreasing from the leading edge to the trailing edge.

For inclination angle $\theta < 10^\circ$, the average Nusselt number for the upper and lower surfaces are expressed in different correlations, whereas for inclination angle $\theta \geq 10^\circ$, it can be expressed as one correlation and the correlation keeps the same as that of a vertical plate if only the gravitational term in the modified Rayleigh number is altered to the component parallel to the inclined surface.

Numerical computations also reveal that as far as the total heat transfer rate is concerned the volumetrically generated heat is transferred to the environment from the upward and downward surfaces equally for inclination angle $\theta \geq 10^\circ$.

References

1. McAdams WH (1954) Heat Transmission. McGraw-Hill Book Company, New York
2. Hatfield DW; Edwards DK (1981) Edge and aspect ratio effects on natural convection from the horizontal heated plate facing downwards. Int J Heat Mass Transfer 24: 1019-1024
3. Clifton JV; Chapman AJ (1969) Natural convection on a finite-size horizontal plate. Int J Heat Mass Transfer 12: 1573-1584

4. **Kierkus WT** (1968) An analysis of laminar free convection flow and heat transfer about an inclined isothermal plate. *Int J Heat Mass Transfer* 11: 241–253
5. **Sparrow EM; Carlson CK** (1986) Local and average natural convection Nusselt numbers for a uniformly heated, shrouded or unshrouded horizontal plate. *Int J Heat Mass Transfer* 29: 369–379
6. **Sparrow EM; Gregg JL** (1956) Laminar free convection from a vertical plate with uniform surface heat flux. *J Heat Transfer* 78: 435–440
7. **Churchill SW; Ozoe H** (1973) A correlation for laminar free convection from a vertical plate. *J Heat Transfer* 95: 540–541
8. **Fujii T; Fujii M** (1976) The dependence of local Nusselt number on Prandtl number in the case of free convection along a vertical surface with uniform heat flux. *Int J Heat Mass Transfer* 19: 121–122
9. **Fujii T; Imura H** (1972) Natural convection heat transfer from a plate with arbitrary inclination. *Int J Heat Mass Transfer* 15: 755–767
10. **Chambers B; Lee T** (1997) A numerical study of local and average natural convection Nusselt numbers for simultaneous convection above and below a uniformly heated horizontal thin plate. *J Heat Transfer* 119: 102–108
11. **Symons JG; Mahoney KJ; Bostock TC** (1987) Natural convection in enclosures with through flow heat sources. *Proceedings of the 1987 ASME-JSME Thermal Engineering Joint Conference*, ASME New York, vol. 2, pp. 215–220
12. **Yang M; Tao WQ** (1995) Three dimensional natural convection in an enclosure with an internal isolated plate. *ASME J Heat Transfer* 117: 619–625